Organic & Biomolecular Chemistry

Cite this: *Org. Biomol. Chem.*, 2012, **10**, 3830

www.rsc.org/obc

PAPER

Water soluble extended naphthalene diimides as pH fluorescent sensors and G-quadruplex ligands†

Filippo Doria,[a] Matteo Nadai,[b] Giovanna Sattin,[b] Luca Pasotti,[a] Sara N. Richter*[b] and Mauro Freccero*[a]

Received 29th November 2011, Accepted 8th March 2012
DOI: 10.1039/c2ob07006e

Extended naphthalene diimides (NDIs) fused to 1,4-dihydropyrazine-2,3-dione, containing two solubilizing moieties, have been synthesized. Fluorescence spectra of the new NDIs were remarkably affected by pH, as the second deprotonation of the dihydropyrazinedione moiety (pK_a 6.9) switched off the emission. Binding to a G-quadruplex folded oligonucleotide and stoichiometry were evaluated by FRET melting assay and CD analysis. G-quadruplex binding was strongly enhanced shifting from pH 7.4 to pH 6.0 as a consequence of the dihydropyrazinedione moiety protonation. Cytotoxicity studies using two human telomerase-positive cell lines (HT29 and A549) revealed that the best G-quadruplex ligand was very active against the colon cell line, with an EC_{50} of 300 nM.

Introduction

Fluorescent molecules have been intensively developed as non-invasive probes for biological applications.[1–4] Of particular interest are those that can reversibly switch between an emitting and a non-emitting state.[5–9] Among them, the pH-responding fluorescent sensors are still holding a prominent position in the current literature, as biochemical processes frequently involve acid–base equilibria with concomitant changes in the pH of the environment.[10–12] Limitations of the available pH probes include low sensitivity, excitation profiles in the ultraviolet region, and a switch of the response at a quite different pH from neutrality. Among the reported sensitive fluorescent probes, core-substituted NDIs (1,4,5,8-naphthalenetetracarboxylic acid diimides)[13] have been thoroughly investigated by Würthner's and Matile's groups as fluorescent dyes, thanks to their remarkably tunable emission properties.[14–18] In particular, they showed that functionalization of the NDI core can induce tuning of the optical and redox properties of this class of dyes extending the range of their application.[19,20] In fact, tri- and tetra-substituted NDIs have recently been exploited as G-quadruplexes (G-4) ligands and cellular fluorescent labelling agents.[21–25] G-4 are DNA secondary structures with a crucial biological role being involved in telomerase maintenance and transcriptional regulation of critical oncogenes.[26,27] The growing interest in biology had propelled the need to develop probes capable of direct detection of G-4 structures *in vivo*.[28–30]

Our interest in substituted NDIs led us to develop a new class of NDIs as G-4 ligands exhibiting absorption and emission properties strongly affected by the surrounding medium (solvent and pH). The first type of these modified T-shaped NDIs (**1** and **2**, Fig. 1) showed strong green fluorescence which could be switched on/off by a pH trigger, but they were not suited for biological application due to negligible solubility in water.[13]

In the current study, we conferred water solubility to the T-shaped NDI core, in order to explore its dual potential as fluorescent probe under physiological conditions and G-4 ligands. Three water-soluble NDIs (**4a–4c**) have been synthesized according to an optimized synthetic protocol. They bear the heterocyclic 2,7-dialkyltetraazabenzo[*e*]pyrene-1,3,6,8,10,11-hexaone core, tethered to two cationic (**4a,b**) or anionic (**4c**) chains at the imide moieties under physiological conditions (Scheme 1).

Results and discussion

The five-steps procedure for the preparation of the T-shaped heterocyclic 2,7-dialkyltetraazabenzo[*e*]pyrene-1,3,6,8,10,11-hexaones **1** and **2** (Fig. 1)[13] has been modified for the synthesis of the water soluble NDIs **4a–c** (Scheme 1). The key-step of these syntheses is a Jones reaction resulting in the oxidation of both the methylene-groups of the amines **3a–c**, without further oxidation of the solubilizing moieties (Scheme 2).

Synthesis

The commercially available anhydride was brominated with dibromocyanuric acid and the resulting product mixture containing the 2,6-dibromo-1,4,5,8-naphthalenetetracarboxylic acid

[a]*Dipartimento di Chimica, Università di Pavia, V.le Taramelli 10, 27100 Pavia, Italy. E-mail: filippo.doria@unipv.it, luca.pasotti@unipv.it, mauro.freccero@unipv.it*
[b]*Dipartimento di Medicina Molecolare, Università di Padova, via Gabelli 63, 35121 Padua, Italy. E-mail: matteo.nadai@unipd.it, giovanna.sattin@unipd.it, sara.richter@unipd.it*

†Electronic supplementary information (ESI) available. See DOI: 10.1039/c2ob07006e

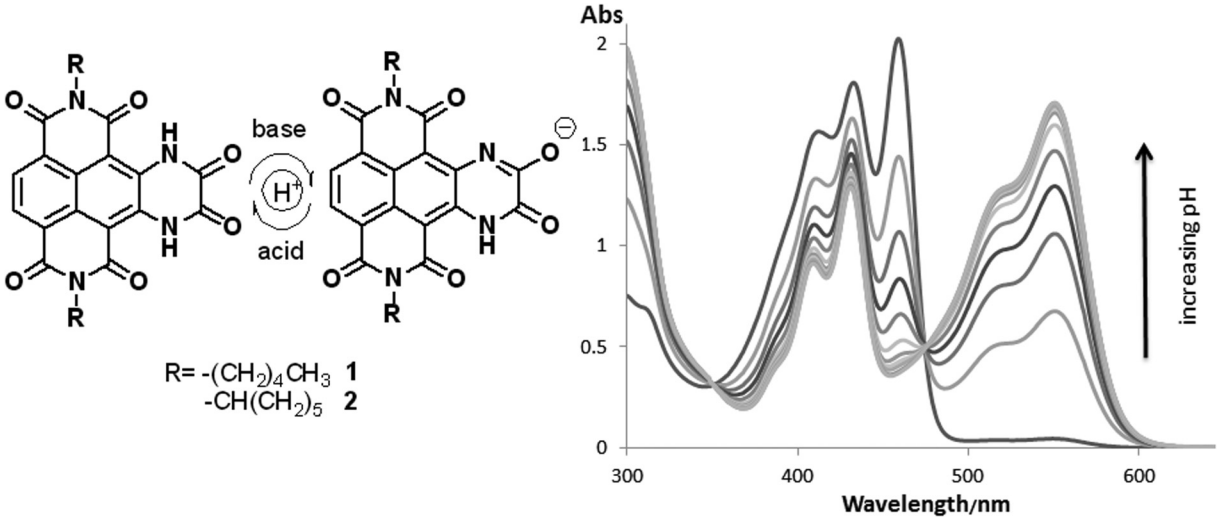

Fig. 1 Structures of T-shaped NDIs (**1** and **2**) fused to a 1,4-dihydropyrazine-2,3-dione exhibiting alkyl moieties. Absorption spectra of the neutral and anionic forms of **1** in DMSO.

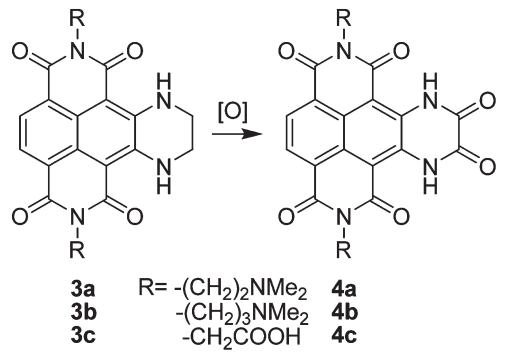

Scheme 1 Generation of the T-shaped heterocyclic 2,7-dialkyltetraazabenzo[*e*]pyrene-1,3,6,8,10,11-hexaones **4a–c** by oxidation.

dianhydride (**5**) was directly used for preparation of the 2,6-dibromo-substituted NDIs (**6a–6c**), synthesized by a classical imidation procedure under acid condition.[31,32] The following nucleophilic aromatic substitution (S_NAr) and subsequent Chichibabin-like ring-closure yielding **7a–c**, were carried out in pure ethylenediamine, at room temperature. Under these mild conditions only a mono-functionalization of the 2,6-dibromo-NDIs was efficiently achieved. Further quantitative mild reductive dehalogenation of **7a–c** was run on the crude reaction mixture, using $Na_2S_2O_4$ dissolved in aqueous DMSO, yielding the diimide analogues **3a–c** in quantitative yields. The final step of the synthesis was carried out using the Jones oxidation protocol, giving **4a–c** in good yield. **8a** was synthesized starting from **7a** according to an identical oxidization protocol.

Spectroscopic properties in organic and aqueous solvents

In order to evaluate the possibility of exploiting the new NDIs as bio-analytical probes, and more specifically as probes for G-4 sensing, we measured the absorbance and emission spectra of the NDIs **4a** and **4c** and their precursors **3a** and **3c**, in organic solvents and water. The disubstituted NDIs **3a** and **3c** were fairly good green fluorescent compounds in water at pH 1 [λ_{em} = 514 nm; fluorescence quantum yield, Φ_{fl}(**3a**) = 0.10] with an absorption spectra characterized by an electronic transition centered at 491 nm. On the contrary, they were very weakly fluorescent in chloroform [λ_{em} = 497 nm; Φ_{fl}(**3a**) = 0.04]. Compared to 2,6-dialkylamino NDIs (λ_{abs} = 620 nm; λ_{em} = 650 nm),[14] the absorption maximum was blue-shifted by more than 130 nm. The UV-Vis absorption of **3a** (λ_{abs} = 491 nm) was slightly more red shifted than that of 2,6-dialkoxy NDIs (λ_{abs} = 470 nm).[14] This evidence suggests that cyclic amine substituents at 2,3 positions on the NDI core are much less efficient electron donors than amine moieties at 2,6 positions, and that **3a** cannot benefit of the cross-conjugation effect on the absorption spectra due to two donors symmetrically located on the NDI core.[17] After oxidation, both UV-Vis spectra of the resulting **4a** and **4c**, were just 30 nm blue-shifted (λ_{abs} = 455 and 453 nm, respectively, in acidic water) in comparison to **3a** and **3c**, in spite of the reduced electron donor properties of the amide *N*-substituent. The UV-Vis spectra of both NDI **4a** and **4c** were investigated in several organic solvents: chloroform, methanol, acetonitrile (ACN), DMSO, acidic water (Fig. 2), and as a function of pH in water (Fig. 3).

The absorbance in organic solvents and in water under very acidic conditions (pH ≤ 1) was only marginally affected by the nature of the solvent (453 < λ_{max} < 461 nm; Fig. 2).

However, absorbance spectra of **4a** in water at higher pH (pH > 1.5) were remarkably different (Fig. 3a and b). In more detail, there was a progressive reduction of the absorbance at the λ_{max} (455 nm) passing from pH 1.5 to pH 4.85 (Fig. 3a), which resemble the behavior of **1** during a titration in DMSO (Fig. 1).[13] In addition, the appearance of a new and red shifted broad band extending up to 580 nm became evident at pH > 6.9 (Fig. 3b).

Both the NDIs **4a** and **4c** exhibited a weak fluorescence emission centered at λ_{em} = 468 nm and 454 nm, respectively, in neat ACN. On the contrary, **4a** and **4c** showed an enhanced light-green fluorescence emission in water solution at pH 1 (Fig. 4), which was five time more intense [Φ_{fl}(**4a**) = 0.54, pH 1, λ_{em} = 458 nm] than the related amine **3a** [Φ_{fl}(**3a**) = 0.10, pH 1; λ_{em}

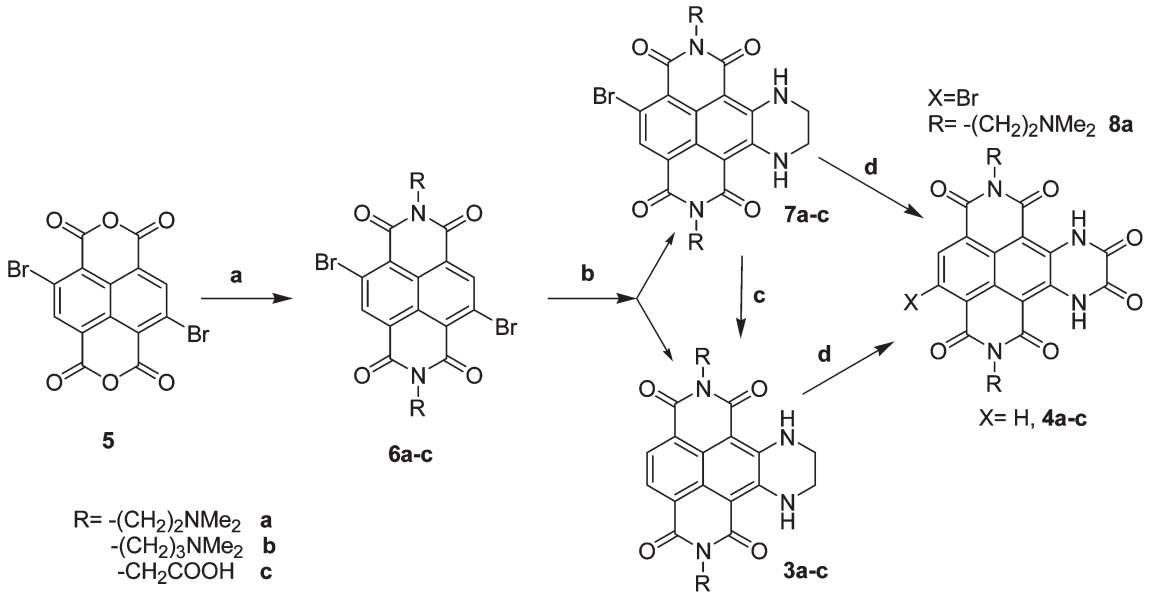

Scheme 2 Reagents and conditions: (a) amines **a–c**, glacial acetic acid, 130 °C, 30 min; (b) ethylene diamine, 25 °C, 16 h, under argon; (c) sodium dithionite, DMSO–H_2O = 20 : 80, 40 °C, 2 h, under argon, (d) $K_2Cr_2O_7$, H_2SO_4, H_2O–acetone, 100 °C, 2 h.

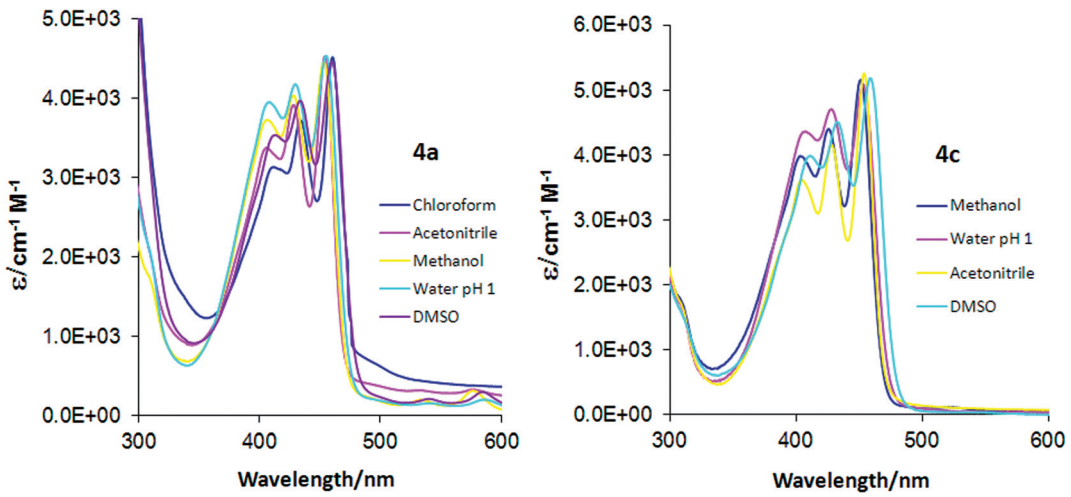

Fig. 2 UV-Vis absorption spectra of **4a** and **4c** in organic solvents and water at pH 1.

479 nm]. Br-NDI **8a** was one of the least fluorescent NDIs [Φ_{fl}(**8a**) = 0.09, pH 1; λ_{em} = 477 nm].

The fluorescence intensity of **4a** monitored at 458 nm slightly decreased at pH higher than 2 (inset B, Fig. 5). The quenching of the emission was more pronounced at 358 nm (inset A, Fig. 5). The emission intensity rapidly dropped at pH above neutrality and it was completely switched off at pH 8.5. The fluorescence intensity raised again at pH higher than 9.0, with a new emission centered at longer wavelength: 535 nm (Fig. 5 and inset C). This new emission became much more intense using an excitation wavelength centered at 458 nm instead of 294 nm (Fig. 6).

Absorbance and fluorescence titration

The mode of protonation/deprotonation of **4a** (Scheme 3) was investigated by spectrophotometric (inset of Fig. 3B and 7A), potentiometric and fluorescence titrations (Fig. 7B). Fluorescence intensity change as a function of pH was analyzed by the Henderson Hasselbalch equation: $\log[(FI_{max} - FI)/(FI - FI_{min}) = pH - pK_a$, where FI is the observed fluorescence intensity at a fixed wavelength, FI_{max} and FI_{min} are the corresponding maximum and minimum respectively. This fluorescence titration yielded a pK_a of 6.88 (Fig. 7B). The UV-Vis titration yielded a very similar pK_a = 6.9 revealing a further additional pK_a = 11.6 (Fig. 7B). Potentiometric titration yielded pK_{a1} = 2.8, pK_{a2} = 7.3 and pK_{a3} = 10.6. The potentiometric pK_a*s* were in fairly good agreement with the pK_a*s* evaluated from fluorescence and spectrophotometric titrations.

Taking into account that (i) the non-water soluble NDI **1**, previously investigated, exhibited a very low pK_a in water–DMSO mixture ($pK_a \sim 1$),[13] and that (ii) the change in the spectrum at 455 nm between pH 1.4 and 5 mimics the behavior of **1** in DMSO (Fig. 1),[13] the pK_{a1} has been assigned to the dissociation

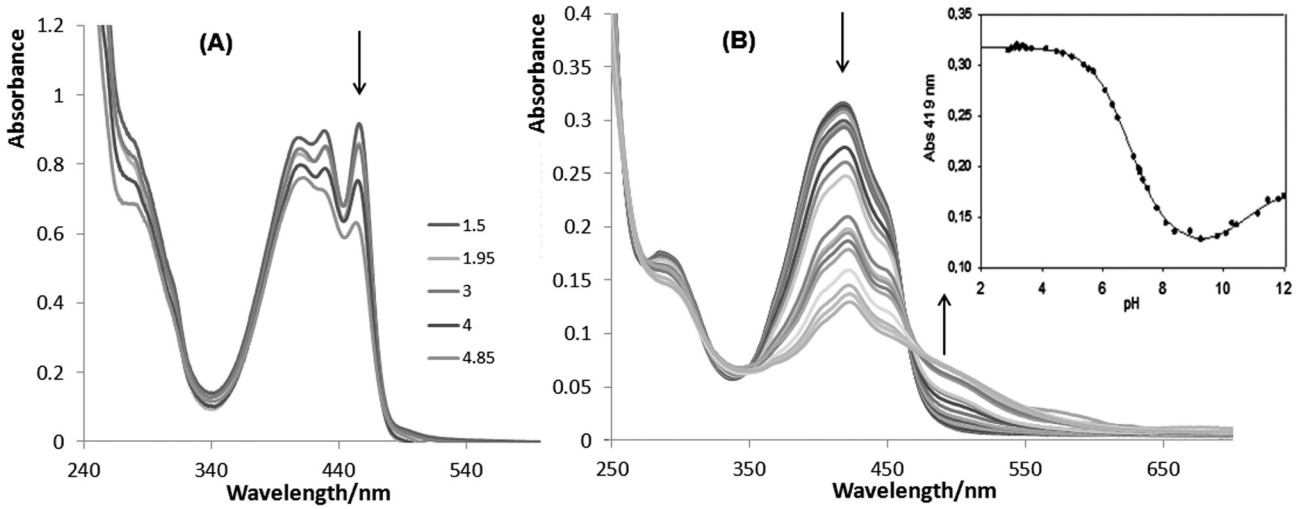

Fig. 3 UV-Vis absorption spectra of compound **4a** in water as a function of pH (A) **4a** (5.1×10^{-5} M) $1.50 < pH < 4.85$ and (B) **4a** (2.0×10^{-5} M), $5.70 < pH < 10.00$. Absorbance monitored at 419 nm as a function of pH is reported in the inset.

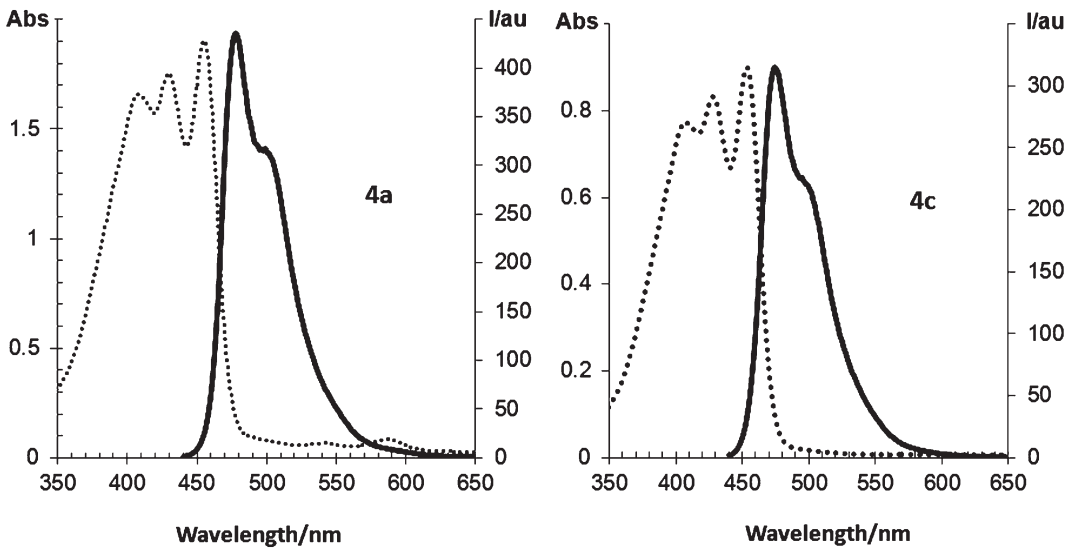

Fig. 4 Absorption (dotted-line) and emission spectra (continuous line) of **4a** and **4c** in water, at pH 1.

of the dicationic **4a-H$_2$**$^+$ (Scheme 3). pK_{a2} should describe the acidity of the second proton of the dihydropyrazinedione moiety. In fact, the deprotonation of **4a-H**$^+$ caused the most significant change in the absorption, as the aromaticity of the resulting **4a-ZW** (or related tautomers) was further extended. Vice versa, the deprotonation of the ammonium moiety should not cause such an extensive change. pK_{a3} should be associated to the deprotonation of the zwitterionic **4a-ZW** (or related tautomers), due to the similar acidity of an alkyl ammonium. The pK_{a2} value suggested that the NDI **4a** should be mainly neutral and non-fluorescent at pH higher than 6.9.

NDIs 4a–c bind G-4 DNA with a preference for the antiparallel conformation, and a 3 : 1 drug–DNA stoichiometry

To evaluate the stabilization of NDI derivatives for telomeric G-4 DNA (hTel), FRET melting experiments were carried out. The increase in the melting temperature (ΔT_m) of the labelled G-4 oligonucleotide by 1.0 μM NDIs **4a–c** was 13.0 ± 0.5 °C, 12.0 ± 1 °C and 3.0 ± 0.5 °C for **4a–c**, respectively. Since **4c** is at least di-anionic at pH 7, it was hypothesized that negative electrostatic repulsion prevented efficient compound binding to the DNA: in fact, when **4c** was incubated with the labelled hTel DNA in the presence of 50 and 100 mM Mg^{2+}, ΔT_m increased by 5.5 and 7.0 °C, respectively.

To check the preferred G-4 conformation stabilized by the best performing compound, **4a**, we carried out CD analysis of the hTel oligonucleotide upon binding with the NDI. **4a** was added before G-4 DNA folding (around 80 °C) and samples were left to equilibrate 24 h prior to CD spectra measurement. In these conditions hTel oligonucleotide alone was present in its mixed antiparallel/parallel form as attested by a major positive peak at 290 nm and a shoulder at 265 nm (Fig. 8a). The addition of compound **4a**, induced a stabilization of the antiparallel G-4

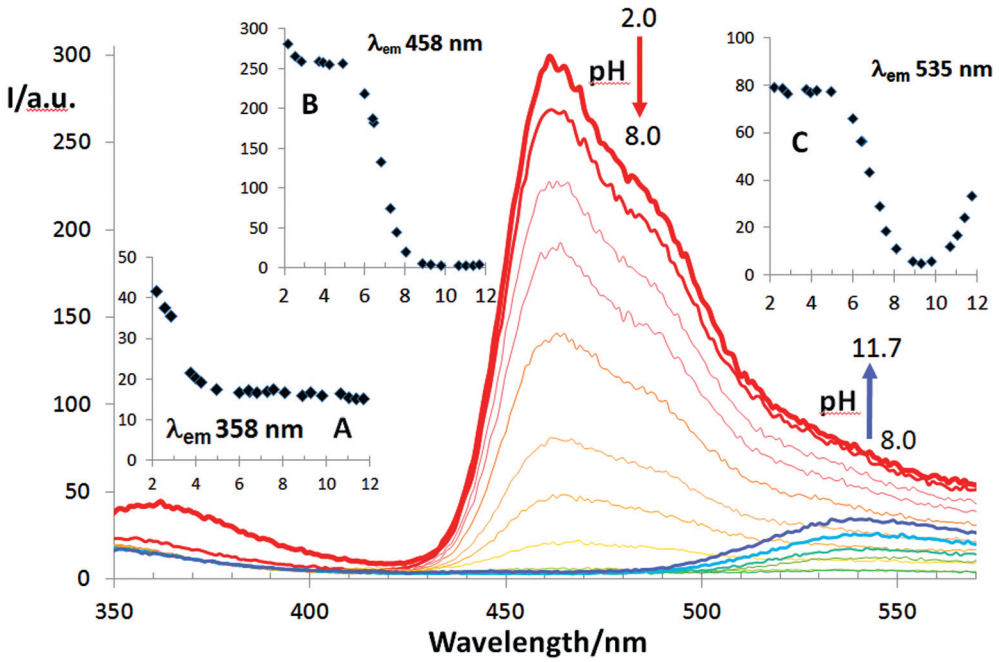

Fig. 5 Fluorescence response of **4a** (2×10^{-5} M) to pH variation at 25 °C in water solution from pH 2 to pH 11.7. Excitation wavelength 294 nm. Inset A, B and C: Fluorescence emissions monitored at 358, 458 and 535 nm, respectively, as function of pH.

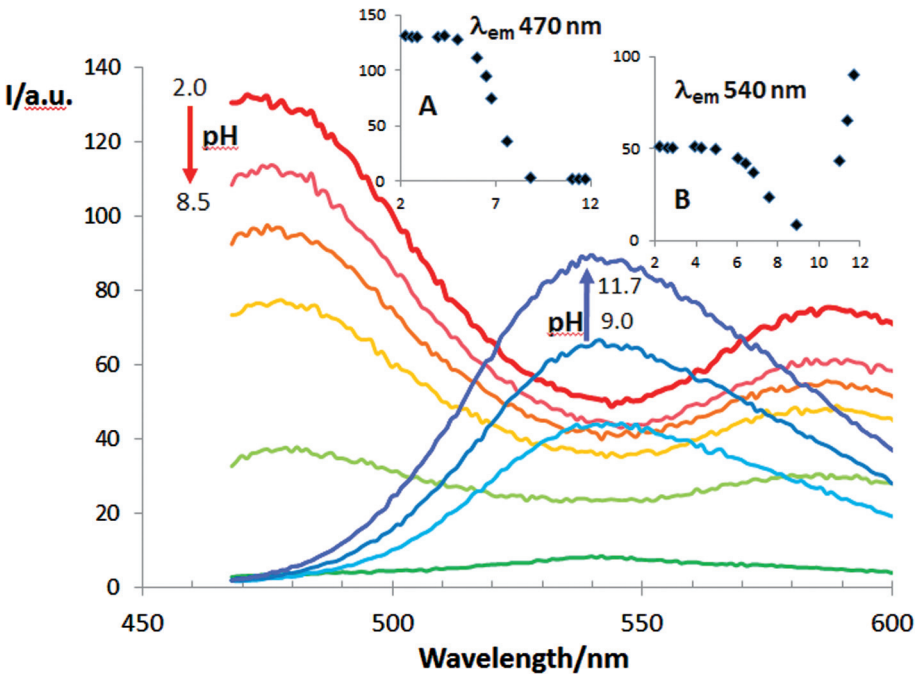

Fig. 6 Fluorescence response of **4a** (2×10^{-5} M) to pH variation at 25 °C in water solution from pH 2 to pH 11.7. Excitation wavelength 458 nm.

structure as proved by an increase in the positive peak at 290 nm (Fig. 8a).

Reaction stoichiometry of compound **4a** against hTel DNA in 10 mM Li cacodylate and 50 mM KCl buffer, at 20 °C, was evaluated by the continuous variation method (Job plot) by mixing DNA and NDI in different proportions, while maintaining constant the whole amount of DNA + NDI. The peak was observed at a DNA fraction of 0.25 which corresponded to a binding stoichiometry of 3 molecules of NDI bound to 1 molecule of DNA (Fig. 8b).

As shown above, pK_{a2} of the dihydropyrazinedione moiety was 6.9, just 0.5 units lower than the pH of our working solutions. We therefore argued that decreasing the pH of the working buffer would augment DNA binding due to reduction of the anion charge on the aromatic core, increasing the population of the monocationic **4a-H**$^+$. To check for binding stability

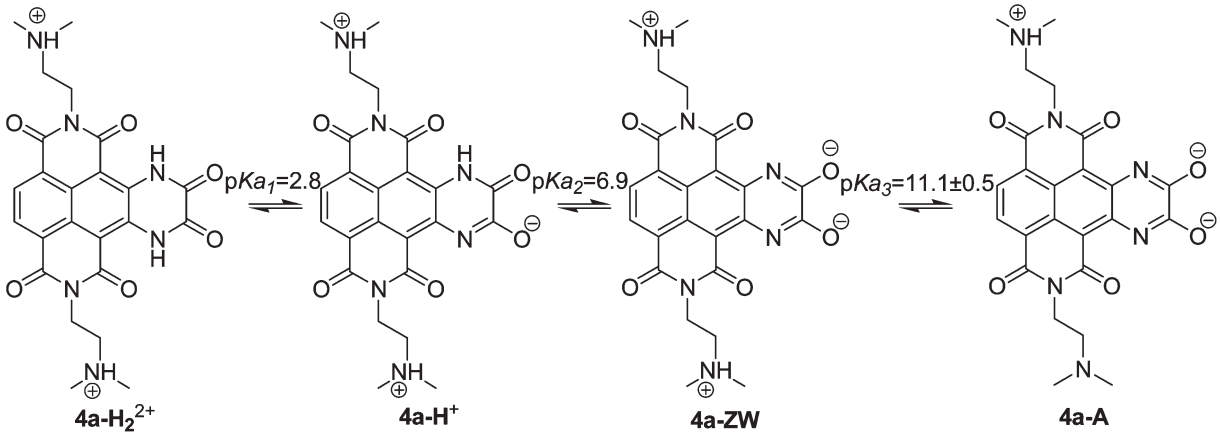

Scheme 3 Acid–base equilibria involving **4a**. Reported pK_a values have been measured by both potentiometric and spectrophotometric titrations at 25 °C. pK_{a3} value is the average of the data from UV-Vis titration (11.6) and potentiometric titration (10.6). For the neutral **4a-ZW** and anionic **4a-A** species, only the most charged structures have been drawn.

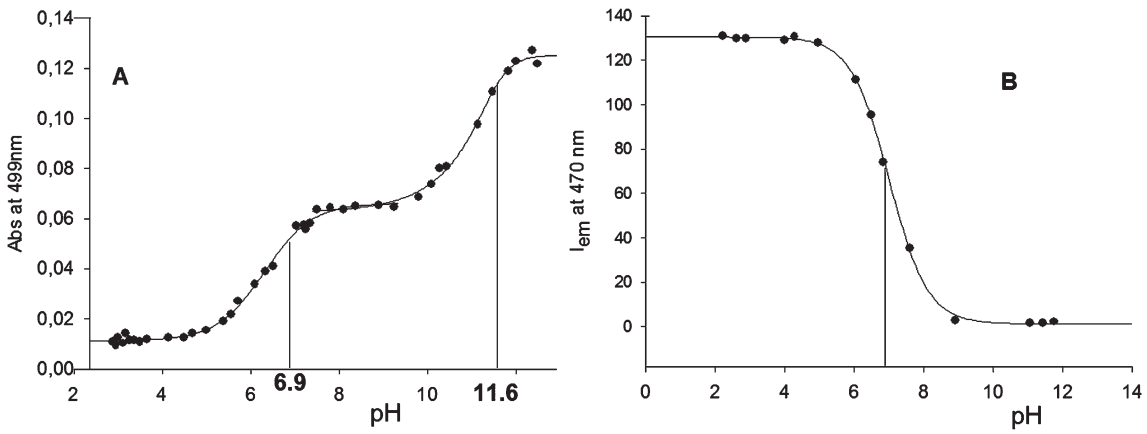

Fig. 7 UV-Vis (A) and fluorescence (B) titrations of **4a** (2×10^{-5} M).

of compound **4a** towards hTel at different pH values, FRET melting assay could not be used due to interference of NDI fluorescence (which increased at lower pH) with the labelled DNA probe. We hence performed CD melting analysis by incubating hTel with or without **4a** at different pH and analyzing molar ellipticity values at 295 nm at increasing temperatures. T_m values were calculated according to the vant'Hoff equation. As shown in Fig. 8c, ΔT_m remarkably increased at lower pH, with a maximum ΔT_m value of 21.2 °C and stabilization at pH 6.0. ΔT_m values above 20 °C indicate good G-4 binders.

The ability of compounds **4a** to enter mammalian cells was tested by confocal microscopy taking advantage of its intense fluorescence emission properties. We observed a significant cell entry and striking accumulation into the nucleus after 30 min exposure (Fig. 9).

Cytotoxicity was next tested against two telomerase-positive human carcinoma cell lines, HT29 and A549 (colon and lung, respectively). Compound **4a** was very active against the colon cell line, with an EC_{50} of 300 nM, and maintained a good activity against lung tumor cells (EC_{50} 1.5 μM). **4b** was slightly less active against both cell lines, with EC_{50} of 3 μM and 6 μM against colon and lung cells, respectively. Remarkably, compound **4a** was one of the most cytotoxic compound among several NDIs developed by our groups[21,22] and in line with NDI cytotoxicity reported by others.[24]

Fluorescence titration

We performed fluorescent titrations to evaluate the effect of hTel interaction on the emission properties of the extended NDI **4a**. Fig. 10 shows fluorescence titration of 0.7 μM **4a** by adding increasing molar ratios of hTel (0–8), at pH 6.0. A 2 fold decrease in fluorescence intensity (FI), monitored at 475 nm, was recorded when hTel was added in equimolar amount. Upon saturation with G-quadruplex DNA photoluminescence from **4a** was quenched.

Conclusion

In summary, our investigation led to the synthesis of three water soluble extended NDIs, with the naphthalene diimide core fused to the heterocyclic 1,4-dihydropyrazine-2,3-dione (**4a–4c**). These NDIs behaved as efficient fluorescent pH sensors in water

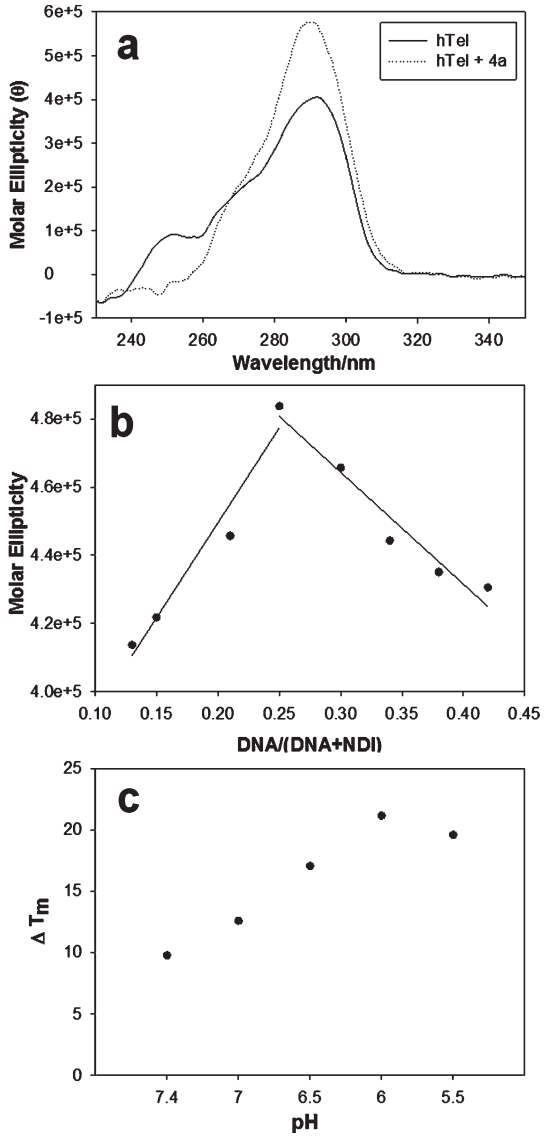

Fig. 8 CD analysis of compound **4a** binding towards hTel. (a) CD spectra of hTel (4 μM) in Li cacodylate buffer (10 mM, pH 7.4) with 50 mM KCl, with (dotted line) or without (solid line) compound **4a** (16 μM); (b) the Job plot performed with a total amount of hTel + **4a** of 10 μM, and varying DNA and drug proportions. The two fitting straight lines intersect at DNA fraction of 0.25, which corresponds to 3 molecules of **4a** bound to 1 molecule of hTel; (c) CD melting analysis of hTel with or without compound **4a** at increasing temperature in 10 mM Li cacodylate buffer, 50 mM KCl, at different pH. T_m values were obtained by plotting molar ellipticities at 295 nm *versus* temperature and fitting with the van't Hoff equation. ΔT_m values were obtained as hTel+**4a** T_m minus hTel T_m values.

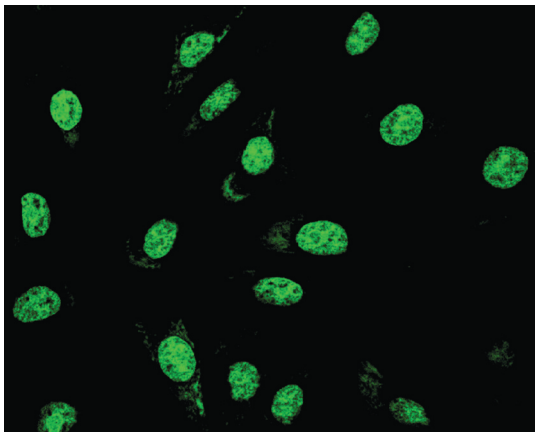

Fig. 9 Cell uptake detection using fluorescence confocal microscopy. Image of **4a** localized in the nucleus after 30 min at 1 μM. Emission was recorded at $\lambda > 470$ nm.

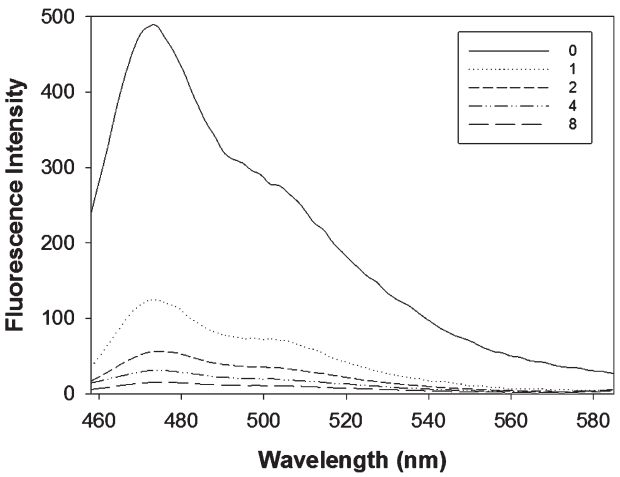

Fig. 10 Fluorescence titration of **4a** (2 μM) by adding increasing molar ratios (as shown in legend) of hTel, at pH 6.0.

solution. Importantly, **4a** exhibited on/off switch of the fluorescence emission between pH 5.0 and pH 8.5, which is appropriate for biological applications. In fact, the monocationic **4a-H**$^+$ acts as a fluorescent weak acid (pK_a = 6.9), but its conjugate base (**4a-ZW**) is a non-fluorescent orange dye. Compound **4a** binding to G-4 folded DNA parallels its emission properties, as both are strongly affected by pH in the neutrality window. It is worthy of note that the monocationic and emitting **4a-H**$^+$ also binds the G-4 DNA much better than its conjugate base **4a-ZW**, due to the favourable electrostatic interaction of the former. Among the NDIs tested, **4a** was identified as a reasonably good G-4 ligand, being able to stabilize G-4 folded DNA with a ΔT_m at 1 μM of 21.2 °C, at pH 6.0, with a preference for the antiparallel conformation, and a 3 : 1 ligand–DNA stoichiometry. Unfortunately, the strong emission of the good G-4 binder **4a**, both at physiological pH and pH = 6, is quenched by the DNA. Work is in progress in order to avoid this fluorescence quenching, by substitutions on the NDI core. Nevertheless, the remarkable cell entry and accumulation into the nucleus of mammalian cells of compound **4a** was detected taking advantage of its intense fluorescence. NDI **4a** was also very cytotoxic towards the colon cell line HT29, with an EC_{50} of 300 nM. This suggests dual potential applications of these extended-NDIs as fluorescence probe and drug candidate.

Materials and methods

The naphthalene bisanhydride were synthesized according to standard published procedures.[32]

To a stirred suspension of dibromodianhydride **5** (600 mg, 0.001 mol) in glacial acetic acid (15 ml) the amine **a**, **b** or glycine (**c**) (0.003 mol) was added. The reaction mixture was stirred at 130 °C, and after 30 min was cooled to r.t., quenched into ice, neutralized with sodium bicarbonate and extracted three times with $CHCl_3$. The organic layer was dried under vacuum to give an orange crude, which was solid purified by column chromatography ($CHCl_3$–MeOH), yielding **6a** (63%), **6b** (58%), **6c** (43%), respectively.

N,*N*′-Di-(*N*,*N*-dimethylethyl)-2,6-dibromonaphthalene-1,4,5,8-tetra-carboxylic acid bisimide (6a)[22,33]

Yellow-orange solid. ^{1}H NMR (200 MHz, $CDCl_3$, 25 °C, TMS). δ = 9.0 (s, 2H); 4.35 (m, 4H); 2.72 (m, 4H); 2.37 (s, 12H). Anal. Calcd for $C_{22}H_{22}Br_2N_4O_4$: C, 46.66; H, 3.92; Br, 28.22; N, 9.89; O, 11.30. Found: C, 46.69; H, 3.89; Br, 28.18; N, 9.92%.

N,*N*′-Di-(*N*,*N*-dimethylpropyl)-2,6-dibromonaphthalene-1,4,5,8-tetra-carboxylic acid bisimide (6b)

Yellow solid. ^{1}H NMR (300 MHz, $CDCl_3$, 25 °C, TMS): δ = 8.7 (s, 2H), 4.65 (m, 2H), 2.49 (m, 4H), 2.28 (s, 12H), 1.95 (m, 4H). Anal. Calcd for $C_{24}H_{26}Br_2N_4O_4$: C, 48.50; H, 4.41; Br, 26.89; N, 9.43; O, 10.77. Found: C, 48.34; H, 4.58; Br, 27.02; N, 9.31. This compound was characterized also as hydrochloride after HPLC purification: *N*,*N*′-Di-(*N*,*N*-dimethylpropyl)-2,6-dibromo-naphthalene-1,4,5,8-tetra-carboxylic acid bisimide (**6b**) 2HCl. ^{1}H NMR (300 MHz, CD_3OD): δ = 8.9 (s, 2H), 4.31 (m, 4H), 3.32 (m, 4H), 2.95 (s, 12H), 2.21 (m, 4H). ^{13}C NMR (CD_3OD): δ = 163.2; 163.0; 139.6; 129.7; 128.9; 127.4; 126.1; 57.1; 43.9; 39.2; 24.8.

N,*N*′-Di-(carboxymethyl)-2,6-dibromonaphthalene-1,4,5,8-tetra-carboxylic acid bisimide (6c)

Grey solid. ^{1}H NMR (300 MHz, DMSO): δ = 8.73 (s, 2H), 4.77 (s, 4H), 2.63–2.48 (m, 4H). ^{13}C NMR (DMSO): δ = 168.6; 160.4; 160.2; 137.7; 131.3; 127.8; 127.2; 127.0; 125.2; 123.9; 47.6. Anal. Calcd for $C_{18}H_8Br_2N_2O_8$: C, 40.03; H, 1.49; Br, 29.59; N, 5.19; O, 23.70. Found: C, 41.15; H, 1.54; Br, 29.21; N, 5.11%.

N,*N*′-Di-(*N*,*N*-dimethylethyl)-6-bromo-5,8,9,10-(1,4-diaza-1,2,3,4-tetrahydroanthracene)tetracarboxylic acid bisimide (7a)

Compound **6a** (200 mg, 0.35 mmol) was placed in a flask containing ethylene diamine (15 ml) and the mixture was stirred at r.t. for 16 h under argon. The resulting red mixture was poured into a solution of HCl (1 N, 100 ml), to induce the precipitation of the product. The collected solid was washed with water and purified by column chromatography ($CHCl_3$) as an orange solid, yield: 78%. ^{1}H NMR (300 MHz, $CDCl_3$, 25 °C, TMS): δ = 10.96 (s, 1H), 10.62 (s, 1H), 8.50 (s, 1H), 4.33 (m, 4H), 3.80 (s, 4H), 2.66 (m, 4H), 2.53 (broad s, 12H). ^{13}C NMR ($CDCl_3$, 25 °C, TMS): δ = 166.0; 165.4; 162.3; 161.3; 144.3; 143.3; 134.3; 131.5; 131.3; 126.9; 126.1; 121.4; 119.9; 97.5; 56.8; 56.5; 45.6; 38.2; 37.9; 29.9. Anal. Calcd for $C_{24}H_{27}BrN_6O_4$: C, 53.05; H, 5.01; Br, 14.70; N, 15.47; O, 11.78. Found: C, 52.90; H, 5.13; Br, 15.00; N, 15.59%.

N,*N*'-Di-(*N*,*N*-dimethylpropyl)-6-bromo-5,8,9,10-(1,4-diaza-1,2,3,4-tetrahydroanthracene)tetracarboxylic acid bisimide (7b)

Orange solid, yield: 69%. ^{1}H NMR (300 MHz, $CDCl_3$, 25 °C, TMS): δ = 10.85 (s, 1H), 10.53 (s, 1H), 8.20 (s, 1H), 4.11 (m, 4H), 3.78 (s, 4H), 2.42 (m, 4H), 2.27 (s, 12H) 1.86 (m, 4H). ^{13}C NMR ($CDCl_3$): δ = 166.0; 165.5; 162.3; 161.3; 144.3; 143.4; 135.0; 131.5; 131.29; 125.1; 122.1; 121.5; 119.9; 97.6; 57.1; 45.1; 29.6; 25.7; 25.5. Anal. Calcd for $C_{26}H_{31}BrN_6O_4$: C, 54.65; H, 5.47; Br, 13.98; N, 14.71; O, 11.20. Found: C, 54.34; H, 5.35; Br, 14.17; N, 14.98%.

N,*N*′-Di-(carboxymethyl)-6-bromo-,5,8,9,10-(1,4-diaza-1,2,3,4-tetrahydroanthracene)tetracarboxylic acid bisimide (7c)

Yellow solid, yield: 65%. ^{1}H NMR (300 MHz, DMSO): δ = 10.89 (s, 1H), 10.60 (s, 1H), 8.54 (s, 1H), 4.72 (s, 4H), 3.72 (s, 4H). ^{13}C NMR (DMSO):δ = 169.3; 169.1; 164.2; 163.7; 161.2; 160.1; 144.7; 143.7; 136.3; 130.0; 129.2; 125.3; 125.0; 120.7; 117.7; 95.3; 53.1; 30.6. Anal. Calcd for $C_{20}H_{13}BrN_4O_8$: C, 46.44; H, 2.53; Br, 15.45; N, 10.83; O, 24.75. Found: C, 46.82; H, 2.43; Br, 15.66; N, 10.71%.

Mild reductive dehalogenation for the synthesis of 3a–3c. General procedure

The reactant **7a–c** (0.07 mmol) was suspended in a solution of 34 ml of DMSO and 6 ml of water, out-gassed by argon and stirred at r.t. Sodium dithionite (0.6 mmol) was added and the new mixture was stirred for 2 h, at 40 °C. After this period the reaction was worked up admitting oxygen atmosphere and was induce the precipitation of the product with water. The resulting suspension was filtered and purified by column chromatography ($CHCl_3$–MeOH = 6 : 4) as a yellow solid.

N,*N*′-Di-(*N*,*N*-dimethylethyl)-5,8,9,10-(1,4-diaza-1,2,3,4-tetrahydroanthracene)tetra-carboxylic acid bisimide (3a)

Yellow-gold solid, yield: 99%. ^{1}H NMR (300 MHz, $CDCl_3$, 25 °C, TMS): δ = 10.60 (s, 2H), 8.30 (s, 2H), 4.37 (m, 4H), 3.80 (s, 4H), 2.74 (m, 4H), 2.45 (s, 12H). ^{13}C NMR ($CDCl_3$, 25 °C, TMS): δ = 166.3; 163.4; 143.9; 124.6; 122.5; 122.2; 56.6; 45.4; 38.1; 37.5; 29.6. Anal. Calcd for $C_{24}H_{28}N_6O_4$: C, 62.06; H, 6.08; N, 18.09; O, 13.78 Found: C, 61.95; H, 6.12; N, 17.98%.

N,*N*′-Di-(*N*,*N*-dimethylpropyl)-5,8,9,10-(1,4-diaza-1,2,3,4-tetrahydroanthracene)tetra-carboxylic acid bisimide (3b)

Yellow-gold solid, yield: 99%. ^{1}H NMR (300 MHz, $CDCl_3$, 25 °C, TMS): δ = 10.64 (s, 2H), 8.15 (s, 2H), 4.20 (m, 4H), 3.80 (s, 4H), 2.41 (m, 4H), 2.30 (s, 12H), 1.85 (m, 4H). Anal. Calcd for $C_{26}H_{32}N_6O_4$: C, 63.40; H, 6.55; N, 17.06; O, 12.99. Found: C, 63.84; H, 6.31; N, 16.95. This compound was characterized also as hydrochloridric salt after HPLC purification: *N*,*N*′-di-(*N*,*N*-dimethylpropyl)-5,8,9,10-(1,4-diaza-1,2,3,4-

tetrahydroanthracene)tetra-carboxylic acid bisimide (**3b**) 2HCl. Orange solid. ^{1}H NMR (300 MHz, CD_3OD): δ = 7.7 (s, 2H), 4.13 (m, 4H), 3.80 (s, 4H), 3.28 (m, 4H), 2.98 (s, 12H), 2.17 (m, 4H). ^{13}C NMR (CD_3OD): δ = 166.9; 164.9; 145.3; 124.6; 123.7; 122.4; 97.6; 57.2; 43.8; 39.2; 38.5; 25.0.

N,*N*′-Di-(carboxymethyl)-5,8,9,10-(1,4-diaza-1,2,3,4-tetrahydroanthracene)tetra-carboxylic acid bisimide (3c)

Yellow solid, yield: 99%. ^{1}H NMR (300 MHz, DMSO): δ = 10.58 (s, 2H), 8.13 (s, 2H), 4.72 (s, 4H), 3.74 (s, 4H). ^{13}C NMR (DMSO): δ = 169.8; 164.7; 162.4; 144.3; 123.5; 122.6; 121.1; 99.1; 95.7; 44.5; 30.7. Anal. Calcd for $C_{20}H_{14}N_4O_8$: C, 54.80; H, 3.22; N, 12.78; O, 29.20. Found: C, 55.01; H, 3.12; N, 12.54%.

Synthesis of 4a–4c, 8a by oxidation. General procedure

The reactant **3a–3c**, **7a** (0.3 mmol) was solved in 30 ml H_2O, 5 ml H_2SO_4 conc. and 5 ml acetone, then was added the $K_2Cr_2O_7$ (200 mg, 0.7 mmol). The brown mixture was reflux for 1 h. After this period the solution become clear, then an additional amount of $K_2Cr_2O_7$ was added, and the solution was heated to reflux. After 2 h the reaction mixture was cooled to r.t., ice and Na_2CO_3 were added, and then it was extracted with $CHCl_3$ (3 × 50 ml). The combined organic phases were washed with brine, dried over $MgSO_4$ and the solvent was removed under vacuum. The crude product was collected and purified by column chromatography ($CHCl_3$).

2,7-*N*,*N*′-Di-(*N*,*N*-dimethylethyl)-4-bromotetraazabenzo[*e*]pyrene-1,3,6,8,10,11-hexaone 2HCl (8a)

Yellow solid, yield: 75%. ^{1}H NMR (300 MHz, CD_3OD): δ = 8.93 (s, 1H), 4.64 (t, J = 5.6 Hz, 4H), 3.62 (t, J = 5.6 Hz, 4H), 3.31 (s, 12H). ^{13}C NMR (CD_3OD): δ = 167.5; 167.0; 163.4; 162.6; 155.0; 138.2; 134.7; 128.0; 127.1; 126.8; 124.6; 120.3; 107.9; 107.4; 57.1; 44.5; 37.3. Anal. Calcd for $C_{24}H_{25}BrCl_2N_6O_6$: C, 44.74; H, 3.91; Br, 12.40; Cl, 11.01; N, 13.04; O, 14.90. Found: C, 44.41; H, 4.02; Br, 12.44; Cl, 11.05; N, 13.12.

2,7-*N*,*N*′-Di-(*N*,*N*-dimethylethyl)-tetraazabenzo[*e*]pyrene-1,3,6,8,10,11-hexaone 2HCl (4a)

Yellow solid, yield: 75%. ^{1}H NMR (300 MHz, CD_3OD): δ = 8.90 (s, 2H), 4.76 (t, J = 5.6 Hz, 4H), 3.75 (t, J = 5.6 Hz, 4H), 3.46 (s, 12H). ^{13}C NMR (CD_3OD): δ = 167.9; 164.6; 155.1; 135.1; 131.3; 127.5; 124.9; 108.0; 57.3; 44.6; 37.2. Anal. Calcd for $C_{24}H_{26}Cl_2N_6O_6$: C, 50.98; H, 4.63; Cl, 12.54; N, 14.86; O, 16.98. Found: C, 51.15; H, 4.48; Cl, 12.24; N, 15.06.

2,7-*N*,*N*′-Di-(*N*,*N*-dimethylpropyl)-tetraazabenzo[*e*]pyrene-1,3,6,8,10,11-hexaone 2HCl (4b)

Yellow solid, yield: 58%. ^{1}H NMR (300 MHz, CD_3OD): δ = 8.80 (s, 2H), 4.31 (m, 4H), 3.70 (m, 4H), 3.30 (s, 12H), 2.71 (m, 4H). ^{13}C NMR (CD_3OD): δ = 166.9; 164.7; 161.8; 155.15; 136.9; 130.9; 127.6; 125.9; 102.0; 57.1; 43.8; 38.3; 25.0. Anal. Calcd for $C_{26}H_{30}Cl_2N_6O_6$: C, 52.62; H, 5.10; Cl, 11.95; N, 14.16; O, 16.18. Found: C, 52.81; H, 5.21; Cl, 12.04; N, 14.04.

2,7-*N*,*N*′-Di-(carboxymethyl)-tetraazabenzo[*e*]pyrene-1,3,6,8,10,11-hexaone (4c)

Yellow solid, yield: 46%. ^{1}H NMR (300 MHz, DMSO): δ = 11.53 (s, 2H), 10.56 (s, 2H), 8.53 (s, 2H), 4.75 (s, 4H). Anal. Calcd for $C_{20}H_{10}N_4O_{10}$: C, 51.51; H, 2.16; N, 12.01; O, 34.31. Found: C, 51.69; H, 2.32; N, 11.83.

Fluorescence spectra were taken on a Perkin-Elmer LS50B spectrofluorimeter. Potentiometric titrations, pH measurements, and electrode calibrations were carried out with a Radiometer TitraLab 90 titration system. Spectrophotometric spectra were taken on a spectrophotometer Varian CARY 100.

Potentiometric titration

A 1 × 10^{-4} M solution (20 mL) of the chosen molecule was prepared in a aqueous/methanol 8/2 solution of 0.05 M $NaNO_3$. The solution was placed in the cell of the automatic titrating system, thermostatted at 25 °C and kept under a N_2 atmosphere. Excess acid (10 μL of 1.00 M standard HNO_3) was added, and the acidic solution was titrated automatically with portions (10 μL) of 0.020 M standard NaOH. The results were obtained as E (potential in mV at the glass electrode) *versus* volume of added base (in mL) and the protonation constants were calculated using the nonlinear fitting program Hyperquad.[34] Before titrations, the cell $E°$ values for the hydrogen glass electrode were determined by means of the Gran method.[35]

Coupled pHmetric–spectrophotometric titration

A 1 × 10^{-4} M solution (20 mL) of the chosen molecule was prepared in an aqueous/methanol 8/2 solution of 0.05 M $NaNO_3$. Excess acid (100 μL of 1.00 M standard HNO_3) was added and the acidic solution was titrated with addition of 0.1 M standard NaOH (100 μL in the ranges of pH 2–4.5, 9.5–12 and 5 μL in the range of pH 4.5–9.5). While the pH was monitored by using a double-electrode pH meter, after each addition of base a portion (3 mL) was withdrawn and placed in a quartz cell to record the absorption spectrum, after which the sample was returned to the bulk solution.

Coupled pHmetric–fluorimetric titration

A 1 × 10^{-5} M solution (20 mL) of the chosen molecule was prepared in an aqueous/methanol 8/2 solution of 0.05 M $NaNO_3$. Excess acid (100 μL of 1.00 M standard HNO_3) was added and the acidic solution was titrated with addition of 0.1 M standard NaOH (100 μL in the ranges of pH 2–4.5, 9.5–12 and 5 μL in the range of pH 4.5–9.5). While the pH was monitored by using a double-electrode pH meter, after each addition of base a portion (3 mL) was withdrawn and placed in a quartz cell to record the fluorescence emissions spectra at three different wavelength of excitation. After which the sample was returned to the bulk solution.

The experimental data of each titration, I_f *vs.* pH and Abs *vs.* pH, were fitted with a sigmoid profile described by equation

$$I_f(\text{or Abs}) = y_0 + \frac{A}{1 + e^{(pH - x_0)/-B}}$$

The parameters '*A*' and '*B*' are related to the height and smoothness of the sigmoidal, y_0 is the initial I_f or Abs, and x_0 represents the pH of the inflection point which fall at a pH value coincident with the pK_a values.

FRET-melting assay

All oligonucleotides were purchased from Sigma-Aldrich (Italy); after an initial dilution at 1 mM in purified water, further dilutions were carried out in the relevant buffer. FRET assay was performed with F21T (5′-d(*FAM*-$G_3[T_2AG_3]_3$-*Tamra*)-3′), with *FAM*: 6-carboxyfluorescein and *Tamra*: 6-carboxy-tetramethylrhodamine. Fluorescence melting curves were determined with a LightCycler II (Roche) real-time PCR machine, using a total reaction volume of 20 µL, with 0.20 µM of tagged oligonucleotide in a buffer containing 10 mM lithium cacodylate pH 7.4 and 50 mM KCl. After a first equilibration step at 30 °C during 2 minutes, a stepwise increase of 1 °C every minute for 65 cycles to reach 95 °C was performed and measurements were made after each cycle with excitation at 470 nm and detection at 530 nm. The melting of the oligonucleotides was monitored by emission of FAM, which was normalized between 0 and 1. T_m was defined as the temperature for which the normalized emission is 0.5. ΔT_m values are mean of 2–3 experiments ± standard deviation.

CD analysis

CD experiments were performed on a Jasco J 810 spectropolarimeter equipped with a NESLAB temperature controller and interfaced to a PC 100. A quartz cuvette with 5 mm path length was used for spectra recorded from 230 to 350 nm at 2 nm bandwidth, 0.1 nm step size, and 4 s time per point. The reported spectrum of each sample represents the average of 2 scans. Observed ellipticities were converted to mean residue ellipticity (θ) = deg × cm^2 × $dmol^{-1}$ (mol. ellip.). The oligomer hTel (5′-d(AGGG[TTAGGG]$_3$)-3′) was diluted from stock to the final concentration (4 µM) in Li cacodylate buffer (10 mM, pH 7.4) with 50 mM KCl and then annealed by heating at 95 °C for 5 min, gradually cooled to room temperature, and incubated at 4 °C overnight. Compounds at 16 µM final concentration were added before hTel annealing. For the CD melting experiments, spectra were recorded from 20 °C to 95 °C, with temperature increase of 5 °C. T_m values were calculated according to the van't Hoff equation, applied for a two state transition from a folded to unfolded state, assuming that the heat capacity of the folded and unfolded states are equal.[36] The binding stoichiometry was determined by the continuous variation method (Job plot). Solutions of hTel and compound **4a** were mixed in different proportions maintaining a total concentration of hTel + **4a** of 10 µM. The mole fractions for DNA/(DNA + NDI) were 0.13, 0.15, 0.21, 0.25, 0.30, 0.34, 0.38, 0.42, 0.50, 0.55. All solutions were prepared in Li cacodylate buffer (10 mM, pH 7.4) with 50 mM KCl. The mole fraction of the DNA was plotted against the molar ellipticity at 290 nm of the DNA–NDI complex. In the plot, the mole fraction of the DNA at which the molar ellipticity of the DNA–NDI complex is maximum, gives the stoichiometry of the complex. The number of NDI binding sites is equivalent to $(1 - x)/x$, where x is the DNA fraction at the intersection of the two fitting straight lines. All samples were allowed to equilibrate overnight. A buffer baseline was collected in the same cuvette and subtracted from the sample spectra. Final analysis of the data was carried out using Excel and Sigma Plot software.

Cytotoxicity

Telomerase-positive human cells were: lung carcinoma cells A549 (ATCC number CCL-185) and human colorectal adenocarcinoma cells HT-29 (ATCC number HTB-38). Cell lines were obtained from American Type Culture Collection (Rockville, MD). Cells were maintained as a monolayer in the logarithmic growth phase at 37 °C in a 5% CO_2 humidified atmosphere, using Dulbecco's modified Eagle's medium supplemented with 10% fetal calf serum and penicillin (100 units mL^{-1})/streptomycin (100 µg mL^{-1}). The cytotoxic effect on tumor cell growth was determined by a MTT assay. NDI compounds were dissolved and diluted into working concentrations with DMSO. Cells (1.75×10^4 cells per well) were plated onto 96-microwell plates to a final volume of 100 µL and allowed an overnight period for attachment. At day 1, 1 µL of each dilution of tested compounds was added per well to get a 1% final concentration of drug solvent per well. Control cells (without any compound but with 1% drug solvent) were treated in the exact same conditions. Cell survival was evaluated by a MTT assay: 10 µL of freshly dissolved solution of MTT (5 mg mL^{-1} in PBS) were added to each well, and after 4 h of incubation, 100 µL of solubilization solution [10% sodium dodecyl sulfate (SDS) and 0.01 M HCl] were added. After overnight incubation at 37 °C, absorbance was read at 540 nm. Data were expressed as mean values of three individual experiments conducted in triplicate. The percentage of cell survival was calculated as follows: cell survival = (*A*well − *A*blank)/(*A*control − *A*blank) × 100, where blank denotes the medium without cells.

For drug uptake experiments, 2.5×10^5 of A549 cells were seeded in a 6-well plate on a coverslip in 2 ml of medium and incubated for 24 hours. The next day cells were treated with compounds and incubated for 30 minutes. The medium was then removed, cells were washed with PBS and fixed by incubation with 2% PFA for 20 min at room temperature in the dark. Subsequently, cells were washed 5 times with PBS, the coverslip mounted on a microscope slide using mounting gel (Vectashield) and sealed. Slides were visualized using a Leica TCS SP2 confocal microscope with a 63× oil submersion lens, excitation wavelength 458 nm and emission range 470–600 nm.

Fluorescence analysis

Compound **4a** was diluted in 10 mM lithium cacodylate pH 6.0 and 50 mM KCl to a final concentration of 2 µM. hTel DNA was

diluted in the same buffer, heated at 95 °C and cooled to r.t. to induce folding. The G-4 folded DNA was added at increasing molar ratios (1, 2, 4 and 8) to the previously prepared solution of compound **4a**. Fluorescence spectra were measured at 25 °C with a LS55 Fluorescence Spectrometer (PerkinElmer), equipped with a temperature controller (FA90, FALC). Spectra were obtained by exciting at 457 nm and read at 465–700 nm with excitation and emission slides of 5 nm. Data were acquired and analysed with FLWinLAb and SigmaPlot software.

Acknowledgements

This work was supported by MIUR, Grant FIRB-Ideas RBID082ATK, Grants AIRC 5826 and 8861 (Associazione Italiana per la Ricerca sul Cancro) and by University of Padua and University of Pavia. We thank Dr L. Mosca (Pavia University) for the potentiometric titrations.

Notes and references

1 T. Mahmood, A. Paul and S. Ladame, *J. Org. Chem.*, 2010, **75**, 204.
2 Y. Liu, Y. Xu, X. Qian, J. Liu, L. Shen, J. Li and Y. Zhang, *Bioorg. Med. Chem.*, 2006, **14**, 2935.
3 D.-M. Kong, Y.-E. Ma, J. Wu and H.-X. Shen, *Chem.–Eur. J.*, 2009, **15**, 901.
4 A.-C. Bhasikuttan, J. Mohanty and H. Pal, *Angew. Chem., Int. Ed.*, 2007, **46**, 9305.
5 S.-V. Bhosale, S.-V. Bhosale, M.-B. Kalyankar and S.-J. Langford, *Org. Lett.*, 2009, **11**, 5418.
6 K. Mohit and G.-J. Subi, *Chem.–Eur. J.*, 2011, **17**, 11102.
7 P. Yang, A. De Cian, M.-P. Teulade-Fichou, J.-L. Mergny and D. Monchaud, *Angew. Chem., Int. Ed.*, 2009, **48**, 2188.
8 A. Granzhan and M.-P. Teulade-Fichou, *Chem.–Eur. J.*, 2009, **15**, 1314.
9 B. Dumat, G. Bordeau, E. Faurel-Paul, F. Mahuteau-Betzer, N. Saettel, M. Bombled, G. Metgé, F. Charra, C. Fiorini-Debuisschert and M.-P. Teulade-Fichou, *Biochimie*, 2011, **93**, 1209.
10 X. Zhang, S. Rehm, M.-M. Safont-Sempere and F. Würthner, *Nat. Chem.*, 2009, **1**, 623.
11 C. Zhou, Y. Li, Y. Zhao, J. Zhang, W. Yang and Y. Li, *Org. Lett.*, 2011, **13**, 292.
12 N.-V. Marinova, N.-I. Georgiev and V.-B. Bojinov, *J. Photochem. Photobiol., A*, 2011, **222**, 132.
13 F. Doria, M. Di Antonio, M. Benotti, D. Verga and M. Freccero, *J. Org. Chem.*, 2009, **74**, 8616.
14 N. Sakai, J. Mareda, E. Vauthey and S. Matile, *Chem. Commun.*, 2010, **46**, 4225.
15 I. Pugliesi, U. Megerle, S.-L. Suraru, F. Würthner, E. Riedle and S. Lochbrunner, *Chem. Phys. Lett.*, 2011, **504**, 24.
16 S.-L. Suraru, U. Zschieschang, H. Klauk and F. Wurthner, *Chem. Commun.*, 2011, **47**, 11504.
17 M. Luo, Q. Wang and Z.-Y. Wang, *Org. Lett.*, 2011, **13**, 4092.
18 M. Jaggi, B. Schmid, S.-X. Liu, S.-V. Bhosale, S. Rivadehi, S.-J. Langford and S. Decurtins, *Tetrahedron*, 2011, **67**, 7231.
19 A. Fin, I. Petkova, D.-A. Doval, N. Sakai, E. Vauthey and S. Matile, *Org. Biomol. Chem.*, 2011, **9**, 8246.
20 F. Wurthner, S. Ahmed, C. Thalacker and T. Debaerdemaeker, *Chem.–Eur. J.*, 2002, **8**, 4742.
21 M. Di Antonio, F. Doria, S.-N. Richter, C. Bertipaglia, M. Mella, C. Sissi, M. Palumbo and M. Freccero, *J. Am. Chem. Soc.*, 2009, **131**, 13132.
22 M. Nadai, F. Doria, M. Di Antonio, G. Sattin, L. Germani, C. Percivalle, M. Palumbo, N.-S. Richter and M. Freccero, *Biochimie*, 2011, **93**, 1328.
23 F. Cuenca, O. Greciano, M. Gunaratnam, S. Haider, D. Munnur, R. Nanjunda, W.-D. Wilson and S. Neidle, *Bioorg. Med. Chem. Lett.*, 2008, **18**, 1668.
24 S.-M. Hampel, A. Sidibe, M. Gunaratnam, J.-F. Riou and S. Neidle, *Bioorg. Med. Chem. Lett.*, 2010, **20**, 6459.
25 M. Gunaratnam, M. de la Fuente, S.-M. Hampel, A. K. Todd, A.-P. Reszka, A. Schätzlein and S. Neidle, *Bioorg. Med. Chem.*, 2011, **19**, 7151.
26 S. Neidle, *FEBS J.*, 2010, **277**, 1118.
27 T. A. Brooks, S. Kendrick and L. Hurley, *FEBS J.*, 2010, **277**, 3459.
28 J. Alzeer, B. R. Vummidi, P. J. C. Roth and N. W. Luedtke, *Angew. Chem., Int. Ed.*, 2009, **48**, 9362.
29 J. Alzeer and N. W. Luedtke, *Biochemistry*, 2010, **49**, 4339.
30 P. Merie, B. Evrard, A. Petitjean, J.-M. Lehn, M.-P. Teulade-Fichou, E. Chautard, A. De Cian, L. Guittat, P. L. Tran, J.-L. Mergny, P. Verrell and A. Tchirkov, *Mol. Cancer Ther.*, 2011, **10**, 1784.
31 C. Roger and F. Wurthner, *J. Org. Chem.*, 2007, **72**, 8070.
32 C. Thalacker, C. Roger and F. Wurthner, *J. Org. Chem.*, 2006, **71**, 8098.
33 F. Doria, M. Nadai, M. Folini, M. Di Antonio, L. Germani, C. Percivalle, C. Sissi, N. Zaffaroni, S. Alcaro, A. Artese, S. Richter and M. Freccero, *Org. Biomol. Chem.*, 2012, **10**, 2798.
34 P. Gans, A. Sabatini and A. Vacca, *Talanta*, 1996, **43**, 1739.
35 G. Gran, *Analyst*, 1952, **77**, 661.
36 N. J. Greenfield, *Nat. Protoc.*, 2006, **6**, 2527.

